Title

DEFLAGRATIONS AND DETONATIONS AS A MECHANISM OF HADRON BUBBLE GROWTH IN SUPERCOOLED QUARK-GLUON PLASMAS

Author

Gyulassy, M.

Publication Date

1983-06-01

LBL-16277
Preprint

Lawrence Berkeley Laboratory
UNIVERSITY OF CALIFORNIA

Submitted to Nuclear Physics B

DEFLAGRATIONS AND DETONATIONS AS A MECHANISM OF HADRON BUBBLE GROWTH IN SUPERCOOLED QUARK-GLUON PLASMAS

M. Gyulassy, K. Kajantie, H. Kurki-Suonio,
and L. McLerran

June 1983

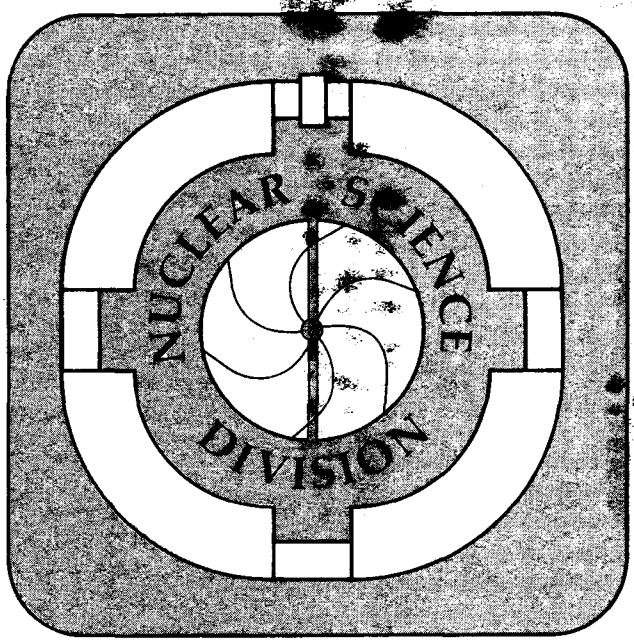

Prepared for the U.S. Department of Energy under Contract DE-AC03-76SF00098

DISCLAIMER

LBL-16277

Deflagrations and detonations as a mechanism of hadron bubble growth in supercooled quark-gluon plasmas

Miklos Gyulassy

Nuclear Science Division, Lawrence Berkeley Laboratory
University of California, Berkeley, CA 94720

K. Kajantie and H. Kurki-Suonio

Department of Theoretical Physics, University of Helsinki
Siltavuorenpenger 20, 00170 Helsinki 17, Finland

and

Larry McLerran

Physics Department, University of Washington
Seattle, WA 98195

Abstract

We discuss the possibility that hadron bubbles formed in quark-gluon plasmas below or slightly above the critical temperature start growing by explosive deflagration or detonation processes. In these the phase transition takes place in a thin layer of discontinuity propagating outward from the point of bubble formation. Combustion theory is written in relativistic form, and possible physical deflagration and detonation bubble solutions conserving energy and momentum, producing entropy, and satisfying correct boundary conditions are classified and numerically discussed using the bag equation of state for quark matter. The implications of these solutions to ultrarelativistic nucleus-nucleus collisions and early cosmology are discussed.

I. INTRODUCTION

One of the remarkable predictions of Quantum Chromodynamics is the existence of a state of matter called the quark-gluon plasma.[1-4] Unlike our familiar hadronic world, the plasma phase is at $T \gg \Lambda_{QCD}$ expected to be extremely simple and well described asymptotically by a Stefan-Boltzmann equation of state. The transition from the hadronic to plasma worlds is expected on general grounds to occur at a temperature $T_c \sim \Lambda_{QCD} \sim 200$ MeV. Recent Monte Carlo lattice calculations[5-12] have made great strides toward clarifying the details of that transition. There is mounting evidence now that this transition is first order.[10-12] In other words, for zero chemical potential it can be characterized by T_c and the latent heat per unit volume $\Delta\varepsilon = \varepsilon_Q - \varepsilon_H \sim \Lambda_{QCD}^4$.

In this paper we consider possible consequences of such a phase transition. In particular, we study the question of whether the latent heat released in the plasma-hadron transition could lead to supersonic, explosive bubbles of hadrons. We have in mind eventual applications to ultrarelativistic nuclear collisions[4,14-19] and to cosmology.[20-22] In cosmology, it is believed that the universe was very homogeneous in the plasma epoch ($t < 1$ μsec). One interesting question is whether the quark to hadron phase transition could have produced large-scale fluctuations that eventually led to the inhomogeneous universe we now observe.[22] In nuclear collisions at very high energies ($E_{lab} > 1$ TeV per nucleon) there is mounting evidence that a transient plasma state could be produced.[4,14-19] One of the most pressing issues in that field is to find conclusive signals for plasma formation.[4] If the transition leads to explosive hadron bubble growth, then there may be striking consequences of the transition for rapidity

correlations, rapidity density fluctuations, azimuthal distributions, and low $P_\perp$ distributions. We return to these applications at the end.

However, the main purpose of this paper is to develop the theory of detonation and deflagration bubbles in this modern context. Figure 1 defines these two phenomena and illustrates the basic difference between them.[23-24] If we imagine at time zero a uniform plasma for $x > 0$, then in both cases the plasma is converted to hadrons along an assumed sharp front. That front eats up the plasma at a constant rate. The difference between deflagration and detonation is the relative flow velocity of the produced hadron matter behind the front. Simply put, deflagration refers to the case in which the hadrons move in opposite direction to the front in the quark matter rest frame. Detonations refer to the case in which the hadronic flow velocity is in the same direction as the front. The assumption that the front has zero width is only a crude approximation. In practice, that width is in order of the reaction mean free paths. For quarks and hadrons $\Lambda_{QCD}^{-1} \sim 1$ fm offers the only scale. Therefore, these idealizations can be expected to apply only to systems of dimensions $R \gg 1$ fm and lifetime $\gg 1$ fm.

The continuity equation of the energy momentum tensor constrains the flow and front velocities as we show in Sect. II. Furthermore, the requirement of positive entropy production greatly constrains the existence of such phenomena as recently emphasized by Van Hove.[25] In the final analysis, the numerical results, of course, depend on the detailed equation of state of both hadronic and quark matter.

In this paper we restrict our study to a general bag-model equation of state because it is simple yet general enough to contain the essential properties of a first-order phase transition. In this model proper energy density $\mathcal{E}$, pressure p, entropy density s of the hadron phase are given by

$$\varepsilon_h = g_1 \frac{\pi^2}{30} T^4 \qquad (1.1),$$

$$p_h = \tfrac{1}{3} \varepsilon_h \qquad (1.2),$$

$$s_h = 4/3\, \varepsilon_h / T \qquad (1.3),$$

as a function of T. For the plasma phase we take

$$\varepsilon_q = g_2 \frac{\pi^2}{30} T^4 + B \qquad (1.4),$$

$$p_q = \tfrac{1}{3} \varepsilon_q - 4/3\, B \qquad (1.5),$$

$$s_q = 4/3\, (\varepsilon_q - B)/T \qquad (1.6),$$

where B is the bag constant. The constants g_1 and g_2 are the degeneracy factors in the two phases. (For n_b boson and n_f fermion states $g = n_b + 7/8\, n_f$.)

This equation of state leads to a first order phase transition at the critical temperature T_c where $p_h = p_q = p_c$ shown in Fig. 2. We define now the critical energy densities $\varepsilon_H = \varepsilon_h(T_c)$ and $\varepsilon_Q = \varepsilon_q(T_c)$ and note that the latent heat per unit volume is just $\Delta\varepsilon = \varepsilon_Q - \varepsilon_H = 4B$ in this model. For $\varepsilon_H < \varepsilon < \varepsilon_Q$ the system is in a mixed phase.

Also illustrated in Fig. 2 are the dashed lines representing superheated hadronic matter and supercooled plasma. These extensions will play a crucial role in the subsequent analysis.

A limitation of our analysis is that we assume the initial plasma is stationary. In both cosmology and nuclear collisions the plasma is always in a state of expansion. This expansion has the effect of curving the detonation and deflagration fronts. For realistic application of our results such expansion effects will eventually have to be included. In this paper we

restrict ourselves to the stationary plasmas to gain basic insight into such explosive processes. Another question we do not discuss is the detailed bubble formation mechanism.[26-27] We just assume a bubble has been formed and study its expansion.

The outline of the paper is as follows: after reviewing relativistic conbustion theory, we discuss the limitations imposed by positive entropy production. We then recover Van Hove's one-dimensional deflagration solutions[25] and show the existence of detonation solutions as well. In Sect. III we construct symmetric deflagration bubble solutions, and in Sect. IV we construct similarity detonation bubble solutions. Finally, concluding remarks, reservations, and future problems are discussed in Sect. V.

II. Relativistic combustion theory

The physical processes we shall discuss in this paper can be described as follows. The system initially consists of supercooled quark-gluon plasma (see Fig. 2) at rest with a uniform energy density ε_2. How this state is attained and how great the supercooling is in cosmology or nucleus-nucleus collisions is a separate dynamical question not discussed in this paper. However, we can motivate the possibility of supercooling at least in nuclear collisions as follows: In the scaling regime[15-18] longitudinal expansion of the plasma leads to rapid cooling, $\varepsilon(\tau) = \varepsilon(\tau_0)(\tau_0/\tau)^{4/3}$, where τ is the proper time. Initially, $\varepsilon(\tau_0) > \varepsilon_\infty$ but at some time τ_Q, $\varepsilon(\tau_Q) = \varepsilon_Q$ (see Fig. 2), and for $\tau > \tau_Q$ the energy density is so small that hadrons begin to form. However, there exists some characteristic proper time $\tau_c \sim \Lambda_{QCD}^{-1} \sim 1\,fm$ for hadrons to be formed in the plasma. Thus, hadrons begin to appear in the plasma only after $\tau > \tau_Q + \tau_0$. By that time, however, the proper energy density is

reduced to $\varepsilon(\gamma_Q+\gamma_0) = \varepsilon_Q(\gamma_Q/\gamma_Q+\gamma_0)^{4/3}$. For the initial energy densities accessible[4] in ultrarelativistic nuclear collisions, $\varepsilon(\gamma_0) \sim (1-4)\,\varepsilon_Q$, it follows that $\varepsilon(\gamma_Q+\gamma_0) \sim \varepsilon_Q/2$. This gives the order of magnitude estimate of how much supercooling may occur in nuclear collisions. For the bag model, with $\varepsilon_Q \sim 4B$, we see in this way that supercooling to $\varepsilon \sim 2B$ may be possible. As the plasma is supercooled it becomes unstable relative to the formation of bubbles of hadron matter.[26-27] Once a bubble has been formed, it can start growing by different means.[27] We shall here study the possibility that the region of hadron matter starts growing away from the point of formation as an explosive process, whereby the phase transition takes place in a layer of negligible thickness propagating outwards. The problem is then to determine the solutions allowed by the laws of relativistic hydrodynamics and the boundary conditions specified by the physical situation. In this section, we shall study the surface of discontinuity in which the phase transition takes place (Fig. 1), and in the following two sections we shall construct the solutions allowed by the assumption of initial homogeneity.

We shall further specialize to a 1 + 1 dimensional situation, i.e., to plane surfaces of discontinuity. The essential coordinates are then only $x^0 = t$ and $x^1 = x$, and the equation of motion of the system is

$$\begin{aligned} \partial_0 T^{00} + \partial_1 T^{10} &= 0 \\ \partial_0 T^{01} + \partial_1 T^{11} &= 0 \end{aligned} \qquad , (2.1)$$

where $T^{\mu\nu}$ is its energy-momentum tensor. Everywhere but on the surface of discontinuity $T^{\mu\nu}$ is assumed to have a perfect fluid form

$$T^{\mu\nu} = T^{\mu\nu}_{(0)} = (\varepsilon + p) u^\mu u^\nu - p g^{\mu\nu} \quad , \qquad (2.2)$$

where

$$u^\mu = (\gamma, \gamma v) \quad ,$$
$$v = v(x,t) = \tanh \Theta(x,t) \quad , \qquad (2.3)$$

is the covariant fluid velocity. To the right (left) of the surface of discontinuity the fluid is assumed to be in the supercooled quark (hadron) phase.

The treatment of the problem can be essentially simplified by going to the frame in which the surface of discontinuity is at rest. The flow in that frame is clearly steady, and the time derivatives in Eqs. (2.1) vanish. They can then be integrated to give T^{01} = constant and T^{11} = constant or

$$(\varepsilon_1 + p_1) \gamma_1^2 v_1 = (\varepsilon_2 + p_2) \gamma_2^2 v_2 \quad ,$$
$$(\varepsilon_1 + p_1) \gamma_1^2 v_1^2 + p_1 = (\varepsilon_2 + p_2) \gamma_2^2 v_2^2 + p_2 \quad , \qquad (2.4)$$

where the notation is as in Fig. 3. From these one can solve

$$(u_1^1)^2 = \sinh^2 \Theta_1 = \frac{(p_1 - p_2)(\varepsilon_2 + p_1)}{(\varepsilon_1 - p_1 - \varepsilon_2 + p_2)(\varepsilon_1 + p_1)} \quad , \qquad (2.5)$$

$$v_1^2 = \frac{(p_1 - p_2)(\varepsilon_2 + p_1)}{(\varepsilon_1 - \varepsilon_2)(\varepsilon_1 + p_2)} \quad , \quad v_2^2 = \frac{(p_1 - p_2)(\varepsilon_1 + p_2)}{(\varepsilon_1 - \varepsilon_2)(\varepsilon_2 + p_1)} \quad . \qquad (2.6)$$

These imply that

$$v_1 v_2 = \frac{p_1 - p_2}{\varepsilon_1 - \varepsilon_2} \quad , \quad (2.7)$$

$$v_1 / v_2 = \frac{\varepsilon_2 + p_1}{\varepsilon_1 + p_2} \quad , \quad (2.8)$$

$$v_{rel} = \frac{v_1 - v_2}{1 - v_1 v_2} = \left[\frac{(p_1 - p_2)(\varepsilon_1 - \varepsilon_2)}{(\varepsilon_1 + p_2)(\varepsilon_2 + p_1)} \right]^{1/2} \quad . \quad (2.9)$$

Defining detonations and deflagrations as in Fig. 3 we have from (2.8) the conditions

$$\begin{aligned} &\text{Detonations} , \quad v_2 > v_1 , \quad \varepsilon_2 - p_2 < \varepsilon_1 - p_1 \\ &\text{Deflagrations} , \quad v_1 > v_2 , \quad \varepsilon_2 - p_2 > \varepsilon_1 - p_1 \end{aligned} \quad . \quad (2.10)$$

The first condition a physical combustion process has to satisfy is that the velocities v_1 and v_2 be physical, i.e., $0 \le v_i^2 \le 1$, $i = 1, 2$. On the $\varepsilon_1, \varepsilon_2$ plane this leads to two disjoint regions, corresponding to detonations and deflagrations. With the bag equation of state ($\varepsilon_2 = \varepsilon_g$, $\varepsilon_1 = \varepsilon_h$, Eqs. (1)-(2)), the velocities are (measuring ε in units of B)

$$v_1^2 = \frac{1}{3} \frac{(\varepsilon_1 - \varepsilon_2 + 4)(3\varepsilon_2 + \varepsilon_1)}{(\varepsilon_1 - \varepsilon_2)(3\varepsilon_1 + \varepsilon_2 - 4)} \quad , \quad (2.11)$$

$$v_2^2 = \frac{1}{3} \frac{(\varepsilon_1 - \varepsilon_2 + 4)(3\varepsilon_1 + \varepsilon_2 - 4)}{(\varepsilon_1 - \varepsilon_2)(3\varepsilon_2 + \varepsilon_1)} \quad , \quad (2.12)$$

which give the regions shown in Fig. 4.

A particularly interesting velocity configuration is that corresponding to the Jouguet condition, $v_1 = v_{s1}$. For the bag equation of state this, using Eq. (2.11) and $v_{s1} = 1/\sqrt{3}$, corresponds to the curves (see Fig. 4)

$$\varepsilon_1 = \varepsilon_2 + 2 \pm 2\sqrt{1+2\varepsilon_2} \qquad (2.13)$$

on the $\varepsilon_1, \varepsilon_2$ plane. One can namely prove that if we fix the initial energy density ε_2 and study the initial velocity v_2 as a function of ε_1, then an extremum of v_2 is obtained when $v_1 = v_{s1}$. To prove this, write $x = v_1 v_2$, $y = v_1/v_2$ and calculate $dv_2^2/d\varepsilon_1$ using $v_{s1}^2 = dp_1/d\varepsilon_1$. This is easily seen to vanish along $xy = v_{s1}^2$, which proves the assertion. Furthermore, along $xy = v_{s1}^2$ one further finds that

$$y^2 \frac{d^2 v_2^2}{d\varepsilon_1^2} = - \frac{2 v_{s1}^2 (\varepsilon_2 + p_2)}{(\varepsilon_1 - \varepsilon_2)^2 (\varepsilon_1 + p_2)^2} (\varepsilon_2 - p_2 - \varepsilon_1 + p_1) \qquad (2.14)$$

Thus, according to (2.10), the extremum is a minimum for detonations and maximum for deflagrations.

The second condition a physical process has to satisfy is that of increasing entropy. This can actually be derived from the equation of motion (2.1) and the laws of thermodynamics. To see this, write

$$T^{\mu\nu} = T^{\mu\nu}_{(0)} + \Delta T^{\mu\nu} \qquad (2.15)$$

where

$$
\begin{aligned}
-\Delta T^{\mu\nu} &= \eta H^{\mu\alpha} H^{\nu\beta} W_{\alpha\beta} + \zeta H^{\mu\nu} \partial_\alpha u^\alpha + \chi (H^{\mu\alpha} u^\nu + H^{\nu\alpha} u^\mu) Q_\alpha \,, \\
H^{\mu\nu} &= u^\mu u^\nu - g^{\mu\nu} \,, \\
Q_\mu &= \partial_\mu T - T u^\alpha \partial_\alpha u_\mu \,, \\
W_{\mu\nu} &= -\partial_\mu u_\nu - \partial_\nu u_\mu + \tfrac{2}{3} g_{\mu\nu} \partial_\alpha u^\alpha \,, \qquad (2.16)
\end{aligned}
$$

and η, ζ, χ are the sheer and bulk viscosities and the heat conductivity. Calculating $u_\mu \partial_\nu T^{\mu\nu}$ one then easily finds

$$
T \partial_\nu (s u^\nu) = - u_\nu \partial_\mu \Delta T^{\mu\nu} \,, \qquad (2.17)
$$

where the right-hand side is responsible for dissipation or entropy production. The form (2.16) for this term is so constructed that entropy is always increasing. Going to the rest frame of the discontinuity surface, where the flow is steady, Eq. (2.17) implies that the condition of entropy increase across the discontinuity is to be formulated as

$$
s_1 u^1_1 \geq s_2 u^1_2 \,. \qquad (2.18)
$$

A physical illustration of this condition is given in Fig. 5. Using Eq. (2.5) this is equivalent to

$$
\frac{s_1^2}{s_2^2} \geq \frac{(\varepsilon_1 + p_1)(\varepsilon_1 + p_2)}{(\varepsilon_2 + p_2)(\varepsilon_2 + p_1)} \,. \qquad (2.19)
$$

Inserting $Ts = \varepsilon + p$, we finally have

$$\frac{s_1}{s_2} \geq \frac{T_1}{T_2} \frac{\varepsilon_1 + p_2}{\varepsilon_2 + p_1}, \quad s = dp/dT, \qquad (2.20)$$

as the entropy condition.

With the bag model equation of state we can express temperatures in terms of energy densities and find that the entropy condition physical processes have to satisfy is

$$\left[\frac{g_1}{g_2} \cdot \frac{\varepsilon_1}{\varepsilon_2 - 1}\right]^{1/2} \geq \frac{3\varepsilon_1 + \varepsilon_2 - 4}{3\varepsilon_2 + \varepsilon_1} . \qquad (2.21)$$

For $\varepsilon_1 = 0$ this demands that $\varepsilon_2 = 4$. Near this end point the condition can be approximated by

$$\sqrt{\varepsilon_1} \gtrsim \left(\frac{g_1}{48 g_2}\right)^{1/2} (\varepsilon_2 - 4) \qquad (2.22)$$

The regions corresponding to physical combustion processes of quark matter to hadron matter are shown in Figs. 6 and 7. One sees that deflagrations are possible even if the quark matter is not quite supercooled; after a deflagration front the hadron matter is in a normal state. Detonations demand more extreme conditions. The initial quark matter must be strongly supercooled and the final hadron matter is left in a strongly superheated state. Note also that the result depends quite strongly on the ratio of the degeneracy factors, as illustrated by Fig. 7.

A special point in Figs. 6-7 is that in which the $\Delta s = 0$ curve meets the boundary of the deflagration region corresponding to $v_1 = v_2 = 0$. Its coordinates in the bag model are (cf. Fig. 2)

$$\varepsilon_1 = 3/(g_1/g_2 - 1) = \varepsilon_H \quad , \qquad \varepsilon_2 = 4 + \varepsilon_1 = \varepsilon_Q \qquad (2.23)$$

This result holds even for a general equation of state: for $p_1 = p_2$ the equality sign in (2.20) implies that also $T_1 = T_2$, i.e., $p_1 = p_2 = p_c$. Another special point is that in which the Jouquet curve $v_1 = v_{1s}$ intersects the $\Delta s = 0$ curve. This corresponds to the maximum value of ε_2 for which deflagrations are possible (Fig. 7).

The regions in the $\varepsilon_1, \varepsilon_2$ plane allowed by the velocity condition but forbidden by the entropy condition for transition from quark matter to hadron matter become physical if we interchange the subscripts 1 and 2 in the entropy condition. Equivalently, we may change the direction of the arrows in Fig. 3, and the processes then become compression or decompression of hadron matter to quark matter (Fig. 6).

As a first application of the results let us consider shocks in quark matter. Shocks are distinguished from combustion processes by the fact that the matter on both sides of the discontinuity surface obeys the same equation of state. With the bag equation of state the entropy condition (2.20) is seen to demand that

$$r \geq \frac{3r^2+1}{3+r^2} \quad , \qquad r = T_1^2/T_2^2 \qquad (2.24)$$

This holds if $T_1 > T_2$, which further implies that $\varepsilon_1 > \varepsilon_2$. Shocks are thus physical if

$$T_1 > T_2 \quad , \quad \varepsilon_1 > \varepsilon_2 \quad , \quad \varepsilon_1 - p_1 > \varepsilon_2 - p_2 \quad , \quad v_2 > v_1 \qquad .(2.25)$$

As a second application, let us consider deflagrations from the surface of quark matter to the vacuum, as described by Fig. 1. Figure 8 shows how the flow velocity (Eq. (2.9)) and the deflagration velocity (v_2 from Eq. (2.6)) depend on the values of ε_2 and ε_1. One can observe the following:

- no supercooling is needed to deflagrations from the surface of quark matter ejecting hadron to vacuum,
- the denser the ejected hadron matter is, the smaller its ejection velocity tends to be,
- the deflagration front propagates extremely slowly into quark matter. The slowness of this flame front calls into question the relevance of this type of surface emission[25] in nucleus-nucleus collisions: the system has disintegrated long before the deflagration front could propagate any appreciable distance.

III. Deflagration bubbles

In the previous section we have studied what happens across a single surface of discontinuity. If we consider the growth of bubbles formed in matter, a single surface of discontinuity is not enough to satisfy the boundary conditions. For symmetry reasons, the produced hadron matter must be at rest while either a single deflagration or detonation front (Fig. 1) leaves the hadrons in motion. To stop the hadrons something must be done, and the simplest possibilities are shown in Figs. 9 and 10.

In case of symmetric deflagration bubbles, the system adjusts the final velocity to zero by sending a supersonic precompression shock into the quark

plasma. This shock compresses the energy density from ε_2 to $\varepsilon_1 > \varepsilon_2$ and accelerates the quark matter to a constant flow velocity v_{fl}. After this a deflagration front moving with a velocity $v_{def} > v_{fl}$ can transform the compressed quark matter to hadron matter of energy density ε_0 and decelerate it to zero velocity. Entropy production across the two fronts is guaranteed by $\varepsilon_1 > \varepsilon_2$ (Eq. (2.25)) and by choosing ε_0 and ε_1 within the physical region in Fig. 6 (with $\varepsilon_2 \to \varepsilon_1$ and $\varepsilon_1 \to \varepsilon_0$).

In case of symmetric detonation bubbles, the primary detonation front causing the phase transition must arrive first (Fig. 9b). Just beyond it, hadronic matter appears superheated to an energy density $\varepsilon_1 > \varepsilon_2$ and moving with sound velocity relative to the detonation front. After that the deceleration to rest takes place via a similarity rarefaction wave, in which both ε and Θ are only functions of $y = \tanh^{-1}(x/t)$ (Fig. 10c and d). The point in which the bubble is formed is always taken as the coordinate origin. The rarefaction zone and the zone of zero hadron velocity are separated by a weak discontinuity moving with sound velocity. No entropy is produced across this discontinuity. These results about detonation bubbles are derived in detail in Sect. IV.

Consider then again deflagration bubbles. The relevant fluid dynamic quantities (Figs. 10a and b) are the energy densities ε_2, ε_1, and ε_0, the deflagration front velocity v_{def}, the shock front velocity v_{sh}, and the compressed quark matter flow velocity v_{fl} (or the corresponding rapidities y_{def}, y_{sh}, y_{fl}). Out of these quantities we shall take the initial quark matter energy density ε_2 as given. Further we have four conditions on the velocities. The first tells that the final hadron matter is at rest, i.e., that the deflagration front velocity is just the back side velocity v_0 calculated from (2.6) (denoted by v_1 there):

$$v_{def}^2 = \frac{(p_1-p_0)(\varepsilon_1+p_0)}{(\varepsilon_1-\varepsilon_0)(\varepsilon_0+p_1)} = \frac{1}{3}\frac{(\varepsilon_1-\varepsilon_0-4)(3\varepsilon_1+\varepsilon_0)}{(\varepsilon_1-\varepsilon_0)(3\varepsilon_0+\varepsilon_1-4)} \quad (3.1)$$

The second tells that the initial quark matter is at rest, i.e., that the shock front velocity is just the front side velocity v_2 calculated from (2.6).

$$v_{sh}^2 = \frac{(p_1-p_2)(\varepsilon_1+p_2)}{(\varepsilon_1-\varepsilon_2)(\varepsilon_2+p_1)} = \frac{1}{3}\frac{3\varepsilon_1+\varepsilon_2-4}{\varepsilon_1+3\varepsilon_2-4} \geq v_s^2 \quad (3.2)$$

The third and fourth conditions tell that the compressed quark matter flow velocity v_{fl} is the relative velocity (2.9) calculated separately across the two fronts:

$$v_{fl}^2 = \frac{(\varepsilon_1-\varepsilon_0)(p_1-p_0)}{(\varepsilon_1+p_0)(\varepsilon_0+p_1)} = 3\frac{(\varepsilon_1-\varepsilon_0)(\varepsilon_1-\varepsilon_0-4)}{(3\varepsilon_1+\varepsilon_0)(\varepsilon_1+3\varepsilon_0-4)} \quad (3.3)$$

$$= \frac{(\varepsilon_1-\varepsilon_2)(p_1-p_2)}{(\varepsilon_1+p_2)(\varepsilon_2+p_1)} = 3\frac{(\varepsilon_1-\varepsilon_2)^2}{(3\varepsilon_1+\varepsilon_2-4)(\varepsilon_1+3\varepsilon_2-4)} < v_{def}^2 \quad (3.4)$$

Imposing the four conditions (3.1-4) leaves us with one degree of freedom not determined by these phase space conditions. We could take this to be v_{def} or ε_0.

To guarantee entropy production across the two fronts, ε_0 and ε_1 have to satisfy (2.21) or lie within the deflagration region in Fig. 6, and ε_1 and ε_2 have to satisfy $\varepsilon_1 > \varepsilon_2$. As ε_1 is an intermediate quantity not of direct interest we eliminate it by using (3.3-4) to express it in terms of ε_0 and ε_2

The possible deflagration bubbles can then be analyzed as shown in Fig. 11. The upper and lower parts of this figure are separated by the line $\varepsilon_2 = \varepsilon_1 + 4$, the straight part of the physical deflagration region in $\varepsilon_0, \varepsilon_1$. Corresponding to each physical point $\varepsilon_0, \varepsilon_1$ we, according to (3.3-4), have a point $\varepsilon_0, \varepsilon_2$ satisfying $\varepsilon_2 < \varepsilon_1$ in the lower part of the figure. In particular, the curved boundary of the lower part is the image of the curved boundary of the upper part. The parameters of physical deflagration bubbles therefore correspond to the lower part in Fig. 11, and Figs. 11a and b show what values of v_{def} and v_{sh} correspond to given $\varepsilon_0, \varepsilon_1$.

Comparing Figs. (8, 11a), we see that the range of allowed deflagration velocities extends to much higher values ($\sim c$) for bubble deflagrations than for surface deflagrations. This is because the flow velocity of the pre-shocked quark matter boosts the small deflagration velocities in Fig. 8. Deflagration bubbles thus have more of a chance of playing a role in nucleus-nucleus collisions.

In general, the numerical values of the parameters have to be studied numerically. A simple analytic approximation can be obtained if we are close to the line separating the two parts in Fig. 11, i.e., $\varepsilon_1 - \varepsilon_0 - 4$ is small. This situation also covers the perhaps most natural phase transition sequence, that in which the phase transition happens by just jumping across the mixed phase from ε_Q to $\varepsilon_H = 3p_c$ with $p = p_c$ in the bag equation of state (Fig. 2), since then $\varepsilon_1 \approx 4 + 3p_c$ and $\varepsilon_0 \approx 3p_c$. A simple calculation gives

$$
\begin{aligned}
v_{def}^2 &= \frac{r}{12}(\varepsilon_1 - \varepsilon_0 - 4) \quad , \quad r = g_1/g_2 \, , \\
v_{fl}^2 &= \frac{r-1}{12r}(\varepsilon_1 - \varepsilon_0 - 4) \quad , \quad v_{def}/v_{fl} = 1 + p_c \, , \\
v_{sh}^2 &= \frac{1}{3} = v_s^2 \quad . \qquad (3.5)
\end{aligned}
$$

The latent heat released in the deflagration process goes into the kinetic energy of the ever-lengthening column of compressed quark matter. To quantify this, let us calculate the total energy E(x) that passes a point x during the deflagration process.

$$E(x) = \int_0^\infty dt \; T^{01}(x,t)$$

$$= x \left(\frac{1}{v_{def}} - \frac{1}{v_{sh}} \right) \gamma_1^2 v_1 (\varepsilon_1 + p_1) \qquad (3.6)$$

As is natural for a similarity solution, this scales linearly with x. The coefficient of proportionality can again be simply approximated in the limit of small $\varepsilon_1 - \varepsilon_0 - 4$:

$$E(x) \approx \frac{4}{3} \; \frac{4 + 3p_c}{1 + p_c} \; x \qquad (3.7)$$

The above results show that expansion via deflagrations is a physically quite appealing candidate solution to the problem of hadron bubble growth in quark matter. Both the initial quark and final hadron energy densities are reasonable. For instance, since

$$B = \left(\frac{B^{1/4}}{200\,\text{MeV}} \right)^4 0.21 \; \text{GeV/fm}^3 \qquad (3.8)$$

the range $\varepsilon_0 < B$ corresponds to hadron matter with the density of nuclear matter or less, for reasonable values of the bag constant B. A slightly problematic feature is the fact that the bubbles grow quite slowly, $v_{def} < v_s$, unless the supercooling is sizable, $\varepsilon_2 \lesssim 2B$.

As emphasized above, these phase space considerations leave one degree of freedom, the deflagration velocity, unspecified (in addition to $\mathcal{E}_2$). The determination of v_{def} will require further dynamical input. For instance, one may study the more microscopic structure of the deflagration front by explicitly using the dissipative terms (2.16). The difficulty here is that one does not know how the response coefficients η, ζ and χ behave near $T = T_c$ and, even more fundamentally, that the discontinuity may be so abrupt that the fluid approach is not at all applicable. This remains an interesting topic of further study.

IV. Detonation bubbles

In the last section we found that we could construct deflagration bubbles by first sending a precompression shock through the quark plasma. To increase entropy, the energy density of the shocked plasma had to be larger than that of the initial plasma. That energy is supplied by the release of latent heat at the deflagration front. The shocked quarks also acquire a net flow velocity. It was possible to bring the hadrons to rest because the deflagration front <u>accelerates</u> the hadrons away from the front. In contrast, a detonation front <u>decelerates</u> the hadrons relative to the quarks. Therefore, a detonation front following a shock cannot bring the hadrons to rest relative to the initial plasma. Suppose we try a solution with a shock following the detonation wave. In that case, the shocked matter is in the hadronic state and we are seeking a way for the hadronic shock front to bring the superheated hadrons to rest. Note from Fig. 6 that the hadronic matter must be highly superheated, $\mathcal{E}_1 \gg \mathcal{E}_H$, right behind the detonation front. Consider a shock wave in that superheated hadronic matter with an energy density to the left of

shock given by ε_0. We saw in Sect. III that positive entropy production across the shock requires that $\varepsilon_0 > \varepsilon_1$. Therefore, the penalty paid for bringing the superheated matter to rest is to heat it up even more. This is clearly undesirable.

To circumvent this problem we seek a solution that leaves the final hadron matter in a cooler normal state, $\varepsilon_0 < \varepsilon_H$. For this purpose, we consider a similarity rarefaction wave behind the detonation front.[23,24] A rarefaction wave allows the superheated hadron matter to cool and expand in a continuous way. The simplest possible rarefaction wave is a similarity wave, i.e., one that depends only on x/t and hence is scale invariant.

To understand similarity rarefaction waves we recall that the hydrodynamic equations ($\partial_\mu T^{\mu\nu} = 0$) can be expressed in this (1 + 1) dimensional case as[18]

$$(\partial_{\hat{t}} + \bar{v}\partial_y)\varepsilon + (\varepsilon + p)(\bar{v}\partial_{\hat{t}} + \partial_y)\theta = 0 \quad , (4.1)$$

$$(\bar{v}\partial_{\hat{t}} + \partial_y)p + (\varepsilon + p)(\partial_{\hat{t}} + \bar{v}\partial_y)\theta = 0 \quad , (4.2)$$

where

$$\hat{t} = \tfrac{1}{2}\log\left(\frac{t^2 - x^2}{r_0^2}\right) \quad , (4.3)$$

$$y = \tfrac{1}{2}\log\left(\frac{t + x}{t - x}\right) \quad . (4.4)$$

Here $\theta(\hat{t}, y)$ is the hydrodynamic flow rapidity and

$$\bar{v}(\hat{t}, y) = \tanh(\theta - y) \quad . (4.5)$$

If we seek scale invariant solutions, then ε, p, θ can be functions of the

"rapidity" y only. In that case eqs. (4.1-2) reduce to

$$\bar{v}\,\partial_y \varepsilon + (\varepsilon + p)\,\partial_y \theta = 0 \quad , (4.6)$$

$$\partial_y p + \bar{v}(\varepsilon + p)\,\partial_y \theta = 0 \quad . (4.7)$$

Noting that $\partial_y p = v_s^2 \partial_y \varepsilon$, where $v_s^2 = \partial p/\partial \varepsilon$, these equations combine to yield

$$(\bar{v}^2 - v_s^2)\,\partial_y \theta = 0 \quad , (4.8)$$

$$v_s^2 \partial_y \varepsilon + \bar{v}(\varepsilon + p)\,\partial_y \theta = 0 \quad . (4.9)$$

Equation (4.8) is solved by θ = const <u>or</u> $\bar{v} = \pm v_s$, i.e.

$$\theta = y \pm y_s \quad , (4.10)$$

where $y_s = \mathrm{th}^{-1} v_s$ is the sound rapidity. If we further specify that $p = v_s^2 \varepsilon$ then eq. (4.9) is solved by ε = const or

$$\varepsilon(y) = \varepsilon(\pm y_s)\, \exp\left[\pm \frac{1 + v_s^2}{v_s} (y \mp y_s)\right] \quad . (4.11)$$

The ± refer to left (+) or right (-) moving similarity rarefaction waves relative to the surrounding fluid.

We can now construct a rarefaction wave joining a region with zero flow rapidity $\theta = 0$ to one with finite flow rapidity right behind the detonation front (located at $y = y_s$) as in Fig. 10c,d. Note that there is a "weak" discontinuity of θ and ε at $y = y_s$. These quantities are continuous across that front but their derivatives are discontinuous. The weak discontinuity propagates in the final hadron rest frame at precisely the speed of sound ($y = y_s$). Furthermore, the velocity of the hadronic matter relative to the detonation front is also the speed of sound since $v_{rel} = \mathrm{th}(\theta(y_{det}) - y_{det}) = v_s$

from eq. (10). We have thus derived fully relativistically the classical Jouguet condition[23,24] for detonations.

The energy density in the hadron matter is then given by

$$\mathcal{E} = \mathcal{E}_1 e^{\frac{1+v_s^2}{v_s}(y-y_{det})} = \mathcal{E}_0 e^{\frac{1+v_s^2}{v_s}(y-y_s)} \quad , \quad (4.12)$$

where by definition, $\mathcal{E}_1 = \mathcal{E}(y_{det})$ and $\mathcal{E}_0 = \mathcal{E}(y_s)$. This solution is shown in Fig. 10d. A qualitative comparison of detonation and deflagration bubbles is seen in Fig. 9.

To fix the value of y_{det} we must join this solution to that of the quark matter across the detonation front. From the detonation conditions derived in Sect. II, we see that y_{def} is just the rapidity of the quark matter in the detonation front rest frame. Therefore

$$y_{det} = \tanh^{-1}\left[v_1 \frac{3\mathcal{E}_1 + \mathcal{E}_2 - 4}{3\mathcal{E}_2 + \mathcal{E}_1} \right] \quad . \quad (4.13)$$

The Jouguet condition requires for similarity rarefaction waves states that the velocity v_1 of the hadrons behind the detonation front is v_s in the front rest frame. This condition led to Eq. (2.13), expressing $\mathcal{E}_1$ in terms of $\mathcal{E}_2$. With Eq. (2.13), we see that y_{det} is now a function of $\mathcal{E}_2$ alone. However, only a limited range of $\mathcal{E}_2$ are allowed by the requirement of positive entropy production. For a fixed degeneracy ratio g_1/g_2, only those $(\mathcal{E}_1, \mathcal{E}_2)$ are allowed that satisfy Eq. (2.21).

Numerical examples of similarity detonation bubbles are shown in Fig. 12 by the dashed line labeled Jouguet detonation. Notice that all detonations involve significantly more supercooling of the plasma than do weak

deflagrations. Nevertheless, both types of solutions leave the final hadronic matter in a cool, normal state. For detonations the rarefaction wave was crucial in obtaining this final state.

Finally, we shall quote a few more results characterizing the detonation bubble solutions. The world line of a fluid element, i.e., the equation of the curve in the similarity rarefaction zone of Fig. 9b, can be obtained by integrating $dx/dt = v(x,t) = \tanh(y - y_s) =$

$$\frac{dx}{dt} = \frac{x/t - v_s}{1 - v_s x/t} \qquad (4.14)$$

If x_0 is the point from which the detonation starts moving the particle, its path is given by

$$t - x = A\,(t+x)^{\frac{1+v_s}{1-v_s}}$$

$$A = \frac{1 - v_{det}}{1 + v_{det}} \left(\frac{1+v_{det}}{v_{det}}\, x_0 \right)^{\frac{-2v_s}{1-v_s}} , \qquad (4.15)$$

and if the particle is pushed to the point x_1, then the relative distance covered by the particle is

$$\frac{x_1 - x_0}{x_0} = \frac{v_s}{1+v_s} \quad \frac{1+v_{det}}{v_{det}} \quad e^{\frac{1-v_s}{v_s}(y_{det} - y_s)} - 1 \qquad (4.16)$$

As we have a similarity solution, this is independent of x_0.

Another quantity of interest is the energy $E(x)$ passing through the point x during the course of the detonation. Calculating as for deflagrations in Eq. (3.6) and using Eq. (4.12) we find

$$E(x) = \int_0^\infty dt\ T^{01}(x,t)$$

$$= x\,\frac{2}{3}\varepsilon_0 \int_{y_s}^{y_{det}} dy\ \frac{\sinh 2(y-y_s)}{\sinh^2 y}\ e^{\frac{1+v_s^2}{v_s}(y-y_s)} \qquad (4.17)$$

As is expected of a similarity solution, this again is linearly proportional to x. The farther away from the start of the explosion one is, the greater is the energy of the explosion.

V. Concluding remarks

In this paper we have developed relativistic combustion theory and found two new solutions corresponding to explosive bubble formation. These correspond to deflagration and detonation processes. The energy fueling these solutions comes from the latent heat liberated in the plasma-to-hadron transitions. The existence of these solutions requires supercooling of the plasma to insure positive entropy production. The main difference between these solutions lies in the way in which the latent heat is used up. In deflagration bubbles the energy is used to preheat and accelerate the quark matter via a shock wave. In detonation bubbles the energy is used to superheat and accelerate hadronic matter. Both solutions lead to "cool" hadronic matter with no flow velocity in a bubble whose radius grows linearly with time. The energy propagates radially outwards in a shell whose thickness also grows linearly with time.

In this section we propose possible consequences of such explosive bubble formation in ultrarelativistic nuclear collisions. In addition, we list key issues that remain unresolved and some problems needing further investigation.

If we accept for the moment that such bubbles can be formed in the expansion phase of nuclear collisions, then what observable consequences may they lead to? As mentioned in Sect. II, the rapid longitudinal expansion of the plasma can easily lead to supercooling of the plasma to $\varepsilon \sim \varepsilon_Q/2$. The transverse rarefaction wave[28] could also help in supercooling the plasma. The seeds for bubble formation could come either from large fluctuations[29] of the initial energy density with respect to the transverse coordinate, high $p_\perp$ hard scattering centers, or the few heavy quarks produced. These bubbles would grow and acquire more energy until they reach the plasma surface. If that surface is a deflagration front as Van Hove suggested,[25] then it is relatively stationary because of the smallness of $v_{def} \sim 0.1$ as shown in Fig. 8. Thus, the bubble can expand until $r \sim R$, the nuclear radius, is reached. As the bubble reaches the surface, the outward-directed energy flux could lead to an azimuthally symmetric blast of hadronic material with mean transverse rapidity, $y_\perp = y_T + y_{fl}$. Here y_T is the mean transverse rapidity due to random thermal motion and y_{fl} is the transverse collective flow rapidity due to the bursting of the bubble. For typical freezeout temperatures $T \sim m_\pi$, $y_T \sim 1.5$. For $y_{fl} \sim (y_{det}$ or $y_{sh}) \sim 1$, we estimate $\langle p_\perp \rangle \sim m_\pi \sinh y_\perp \sim 1$ GeV/c, which is significantly larger than usual hadronic $\langle p_\perp \rangle \sim 0.4$ GeV/c. The azimuthal symmetry may not be perfect for bubbles produced at finite transverse coordinate. However, it would be easy to distinguish such bubbles from normal jets by correlating the magnitude ot the <u>total</u> transverse energy per unit rapidity, $dE_\perp/dy$, with the azimuthal asymmetry. Normal jets with the same $dE_\perp/dy$ would be much more asymmetric in ϕ. Multiple medium $p_\perp$ jets could be ruled out if the rate of bubble formation is larger than the predicted multi jet rate.

A second important feature of bubble growth is its localization in rapidity space. Consider a bubble formed at $\tau = \tau_0$, $x = x_0$, $t = (\tau_0^2 + x_0^2)^{1/2}$ in a particular frame. The bubble front cannot arrive at the original $z = 0$ before $t_c = t_0 + z_0$. However, if $t_c > R\sqrt{3}$ then the transverse rarefaction wave[28] will have passed through the center of the plasma at $z = 0$, and the conditions for bubble growth may no longer hold. Thus, z_0 must be close enough to the origin that $t_c < R\sqrt{3}$. Since the rapidity of the bubble center is $y_0 = \ln(t_0 + z_0/\tau_0)$, $t_c < R\sqrt{3}$ implies that $y_0 < \ln R\sqrt{3}/\tau_0$. Thus, the total rapidity width influenced by a bubble is $\Delta y \lesssim 2 \ln R$. Bubble growth in heavy nuclear collisions may thus lead to medium-range rapidity correlations with $\Delta y \sim 2-4$.

We also note that bubble production leads to extra entropy productions. Since the rapidity density dN/dy reflects the entropy density,[30] bubble formation could lead to enhanced rapidity density fluctuations. The magnitude of the enhancement depends, of course, on the degree of supercooling. In addition, if multiple bubbles are produced within $\Delta y \sim 2 \ln R$ of each other, then the bubble walls could collide and lead to even greater entropy production in a narrow rapidity band.

In summary, we propose three observable consequences of explosive bubble formation in supercooled plasmas: (1) large dE_T/dy correlated with near azimuthal symmetry, (2) medium-range rapidity correlations growing as $\Delta y \sim 2 \ln R$, and (3) enhanced rapidity density fluctuations. We note, furthermore, that such phenomena may have been observed already in some cosmic-ray events.[31] For example, in the Concord event anomalous fluctuations in the pseudo-rapidity distribution is correlated with medium $p_\perp \sim 0.5$-1 GeV/c and approximately azimuthal symmetry. In the Texas Lone Star event large rapidity fluctuations are also seen. On the other hand, two

very high energy nuclear collision events reported by the JACEE collaboration[32] have smaller rapidity density fluctuations. The Centauro and Chiron events exhibit an unusually large $p_\perp$ distribution of secondaries. Perhaps these features are related to detonation waves. Clearly, much more data are required before any conclusions can be drawn.

While the above proposed consequences of bubble growth are plausible, many theoretical issues remain unresolved at present. Serious application of combustion phenomena to nuclear collisions or cosmology must await resolution of the following problems:

1. On the technical side the effect of finite chemical potentials and more realistic equations of state need to be explored. Also, we have only considered 1 + 1 dimensional combustions. The full 3D spherical symmetric bubble solutions need to be investigated. That 3D bubbles could behave differently from 1D bubbles can be anticipated from the observation[33] that 3D deflagration fronts in chemical explosions are unstable and that flames actually propagate in a turbulent rather than simple hydrodynamical manner. The same mechanism may operate in quark-gluon plasmas.
2. Bubble growth in expanding systems needs study. In general, expansion will lead to curved shock and flame fronts in Fig. 9. Where these curved fronts intersect a critical curve $\Upsilon = L_c \sim R\sqrt{3}$ will determine the extent of the medium-range rapidity correlations.
3. The nature of the seeds for bubble formation needs investigation. If fluctuations in the energy density indeed provide the seeds, can flame fronts propagate in unhomogeneous plasmas? What is the probability of forming a bubble?

4. Can local thermal equilibrium be achieved and maintained on both sides of the flame front? Naively, we expect that if the relevant mean free paths are small compared to the dimension of the system ($\lambda \ll R$), then local thermal equilibrium can be maintained. However, Van Hove conjectured[25] that quasi equilibrium may also be reached at early times if we concentrate on inclusive observables. For nuclear collisions, longitudinal expansion leads to rapid time variations, $\partial \ln \varepsilon / \partial \tau \propto \tau^{-1}$, independent of the transverse dimension. Ideal hydrodynamics requires $\lambda \ll (\partial \ln \varepsilon / \partial \tau)^{-1}$. Simple estimates[1] give $\lambda \propto (\alpha^2 T)^{-1} \sim \tau/\alpha^2$, where α is the effective strong coupling. If $\alpha^2 \ll 1$, then transport corrections to ideal hydrodynamics are required. Flame propagation may thus have to be studied via the Navier-Stokes equation (eq. (2.15)-(2.17)) due to the rapid longitudinal expansion even for very large nuclei.

5. The thickness of the flame front will in any case require solution of the Navier-Stokes equations. In the nonrelativistic case,[23] it is known that the thickness depends on both the chemical reaction rate and the thermal conductivity of the system. For the plasma, there is considerable uncertainty in the reaction rate. Naively, we guess that $\Lambda_{QCD}^{-1} \sim 1$ fm/c provides the only natural time scale. However, the problem here is how long does it take for the nonperturbative vacuum fluctuations to re-establish themselves in the presence of quark-gluon plasma. Even if Λ_{QCD}^{-1} is the final answer, then we are faced with the problem that time variations due to longitudinal expansion are initially on the same order. Thus, the idealization of thin flame fronts may be too crude.

6. What happens when the flame front hits the plasma surface How does the energy flux get transformed into produced hadrons What is the influence of the transverse rarefaction wave on the bubble growth Observable consequences of explosive bubbles depend on the resolution of these questions.
7. Probably the most basic and difficult question is whether the extreme supercooling of the plasma can actually occur. It could be that the required metastable supercooled and superheated phases do not exist! Or, if they exist, the barrier between them could be too large. At this time, even the relevant order parameters characterizing these phases are poorly understood. The detonation bubbles are especially vulnerable to uncertainties about the superheated hadronic phase.

Given the above uncertainties and reservations, great care must be exercised in applying these bubble solutions. Nevertheless, they may provide a hint that novel bulk phenomena could occur in quark-gluon plasmas. If explosive bubble growth does occur, the resulting striking signatures could provide diagnostic information on the properties of that plasma.

Acknowledgements

Two of us (M.G., K.K.) thank Prof. L. Van Hove for very instructive discussions and for describing his results[25] before publication. One of us (L. Mc.) also thanks J. Iwai, J. Lord, J. Wilkes for discussions on signatures. This work was supported in part by the Director, Office of Energy Research, Division of Nuclear and High Energy Physics of the U.S. Department of Energy under Contract DE-AC03-76SF00098 and DE-AC06-81ER40048.

References

[1]E.V. Shuryak, Phys. Repts. 61, 71 (1980).

[2]D. Gross, R. Pisarski, and L. Yaffe, Rev. Mod. Phys. 53, 43 (1981).

[3]H. Satz (Ed.), Statistical Mechanics of Quarks and Hadrons, North Holland Publ. Co., 1981.

[4]M. Jacob and H. Satz (Eds.), Quark Matter Formation and Heavy Ion Collisions, World Scientific Publishing Co., Singapore, 1982.

[5]L. McLerran and B. Svetitsky, Phys. Lett. 98B, 195 (1981); Phys. Rev. D24, 450 (1981).

[6]J. Kuti, J. Polonyi, and K. Szlachanyi, Phys. Lett. 98B, 199 (1981).

[7]K. Kajantie, C. Montonen, and E. Pietarinen, Zeitschrift fur Physik C9, 253 (1981); I. Montvay and E. Pietarinen, Phys. Lett. 115B, 151 (1982).

[8]J. Engels, F. Karsch, I. Montvay, and H. Satz, Nucl. Phys. B205 [FS5], 545 (1982); J. Engels, F. Karsch, and H. Satz, Phys. Lett. 113B, 398 (1982); J. Engels and F. Karsch, CERN preprint (Ref. TH. 3481), Dec. 1982.

[9]J. Kogut, M. Stone, H.W. Wyld, W.R. Gibbs, J. Shigemitsu, S.H. Shenkar, and D.K. Sinclair Phys. Rev. Lett. 50, 393 (1983).

[10]L.G. Yaffe and B. Svetitsky, Phys. Rev. D26, 963 (1982); Nucl. Phys. B210, 423 (1982).

[11]T. Celik, J. Engels, and H. Satz, Bielefeld preprint (BI-TP83/04), March 1983.

[12]J. Kogut, H. Matsuoku, M. Stone, H.W. Wyld, S. Shenkar, J. Shigemitsu, and J.K. Sinclair, Urbana Preprint ILL-(TH)-83-9, April 1983.

[13]P. Steinhardt, Phys. Rev. D25, 2074 (1982).

[14]R. Anishetty, P. Koehler, and L. McLerran, Phys. Rev. D22, 2793 (1980).

[15]J.D. Bjorken, Phys. Rev. D27, 140 (1983).

[16]K. Kajantie and L. McLerran, Phys. Lett. 119B, 203 (1982); Nucl. Phys. B214, 261 (1983).

[17]K. Kajantie and R. Raitio, Phys. Lett. 121B, 415 (1983).

[18]K. Kajantie, R. Raitio, and P.V. Ruuskanen, Nucl. Phys. B222, 152 (1983).

[19]M. Gyulassy, Nucl. Phys. A400, 31c (1983).

[20]K.A. Olive, Nucl. Phys. B190, 483 (1981).

[21]E. Suhonen, Phys. Lett. 119B, 81 (1982).

[22]M. Crawford and D.N. Schramm, Nature 298, 538 (1982).

[23]R. Courant and K.O. Friedrichs, Supersonic Flow and Shock Waves, Springer Verlag, 1976.

[24]L.D. Landau and E.M. Lifshitz, Fluid Mechanics, 120-123, Pergamon Press, 1959.

[25]L. Van Hove, CERN TH.3592 (1983) preprint.

[26]L.D. Landau and E.M. Lifshitz, Statistical Physics, Part 1, 162, Pergamon Press, 1980.

[27]E.M. Lifshitz and L.P. Pitaevskii, Physical Kinetics, 99, Pergamon Press, 1981.

[28]G. Baym, J.P. Blaizot, W. Czyz, B.L. Friman, and M. Soyeur, Urbana preprint (1983).

[29]H. Ehtamo, J. Lindfors, and L. McLerran, Helsinki HU-TFT-83-1 preprint (1983).

[30]M. Gyulassy and T. Matsui, LBL-15947 preprint (1983).

[31]J. Iwai, et al., Prog. Theor. Phys. 55, 1537 (1976); Nuovo Cim. 69A, 295 (1982).

[32]JACEE collaboration, T. H. Burnett, et. al., Phys. Rev. Lett. 50, 2062 (1983).

[33]G. Andrews, D. Bradley, and S. Lwakabama, Combustion and Flame 24, 285 (1975).

Figure Captions

Fig. 1. Space-time development of one-dimensional deflagration and detonation fronts converting quark-gluon matter, Q (dotted lines), into hadronic matter, H (dashed lines).

Fig. 2. Schematic diagram of energy density and pressure p as a function of temperature (for zero chemical potential). At T_c, the pressures in the two phases are equal, but there is a latent heat per unit volume $\varepsilon_Q - \varepsilon_H$. The dashed curves indicated the state of superheated hadronic matter and supercooled quark matter.

Fig. 3. Fluid variables in the rest frame of the discontinuity. The difference between detonations and deflagrations is in the relative magnitude of the velocities.

Fig. 4. Kinematic domains in which the continuity equations can be satisfied with physical flow velocities $0 \leq v_i^2 \leq 1$ in both hadron and quark phases. Dashed lines (Eq. (2.13)) correspond to the Jouguet condition, in which the hadron flow velocity is equal to the sound velocity in hadronic matter.

Fig. 5. Schematic diagram illustrating how entropy can increase across a deflagration front due to increased volume in hadronic phase in spite of the reduction of the internal energy density $\varepsilon_1 < \varepsilon_2$.

Fig. 6. Positive rate of entropy production restricts deflagrations and detonations in the quark phase to domains in $(\varepsilon_1, \varepsilon_2)$ indicated. The $\Delta S = 0$ curve is calculated for $g_1/g_2 = 2/3$ for illustration. Above that curve Q → H discontinuities lead to negative entropy production. However, H → Q discontinuities (compression or decompression) lead then to positive entropy production.

Fig. 7. Curves of $\Delta S = 0$ for different degeneracy ratios in the bag model. The dashed curves correspond to the Jouguet condition.

Fig 8. The dependence of v_{defl} (the velocity with which the deflagration front penetrates quark-gluon plasma of energy density $\mathcal{E}_2$) and v_{out} (the velocity with which hadron matter at energy density $\mathcal{E}_1$ is ejected out of the surface) on $\mathcal{E}_2$ and $\mathcal{E}_1$ with the bag equation of state. Physical surface deflagrations are allowed only in the region bounded by $\mathcal{E}_2 = \mathcal{E}_1 + 4\mathcal{B}$ and the upside-down parabolic curve marked with fixed g_1/g_2 values. Degeneracy ratios g_1/g_2 closer to unity allow a greater physical domain. The positive parabolic curves of constant v_{defl} show that physical deflagration velocities are very small. The hadron ejection velocities as shown by the vertical rays extend to high velocities.

Fig. 9. Space-time growth of hadron bubble via deflagration front following precompression shock (a) or via detonation front followed by rarefaction wave (b). The weak discontinuity at the rarefaction front moves with the speed of sound. Paths of quarks and hadrons indicated by dotted and dashed lines, respectively. Both solutions are symmetric and scale invariant. See Fig. 10 for detailed flow characteristics.

Fig. 10. Flow rapidity Θ ($= \text{th}^{-1} v_{fl}$) and proper energy density $\mathcal{E}$ as a function of $y = \text{th}^{-1}(x/t)$ for symmetric deflagration (a,b) and detonation (c,d) bubbles as in fig. 9. The rapidity of the deflagration (detonation) fronts are indicated by y_{def} (y_{det}). The precompression shock rapidity is y_{sh} and the rapidity of sound is y_s ($v_s = \text{th}\, y_s$). Note that in detonations superheated hadronic matter replaces the preheated quark matter in the transition region in which $\Theta > 0$.

Fig. 11. Symmetric deflagration parameters. The figure is divided into two parts by the straight line $\varepsilon = \varepsilon_0 + 4B$ (thick line). For $\varepsilon > \varepsilon_0 + 4B$ the ordinate is the proper energy density ε_1 of the preheated quark matter. For $\varepsilon < \varepsilon_0 + 4B$ the ordinate is the energy density ε_2 of the initial supercooled quark matter. The abscissa is the energy density ε_0 of the hadron matter formed. The curves correspond to curves of constant deflagration front velocity, v_{def}, in part (a) and to constant shock velocity, v_{sh}, in part (b). The domains allowed by $\Delta S \geq 0$ are bounded by curves marked with appropriate values of g_1/g_2.

Fig. 12. The initial quark energy density, ε_2, versus final hadronic energy density, ε_0, for symmetric weak deflagration (v_{def}) and Jouguet detonation bubbles. Note that detonation requires significantly more supercooling of quark matter than does deflagration.

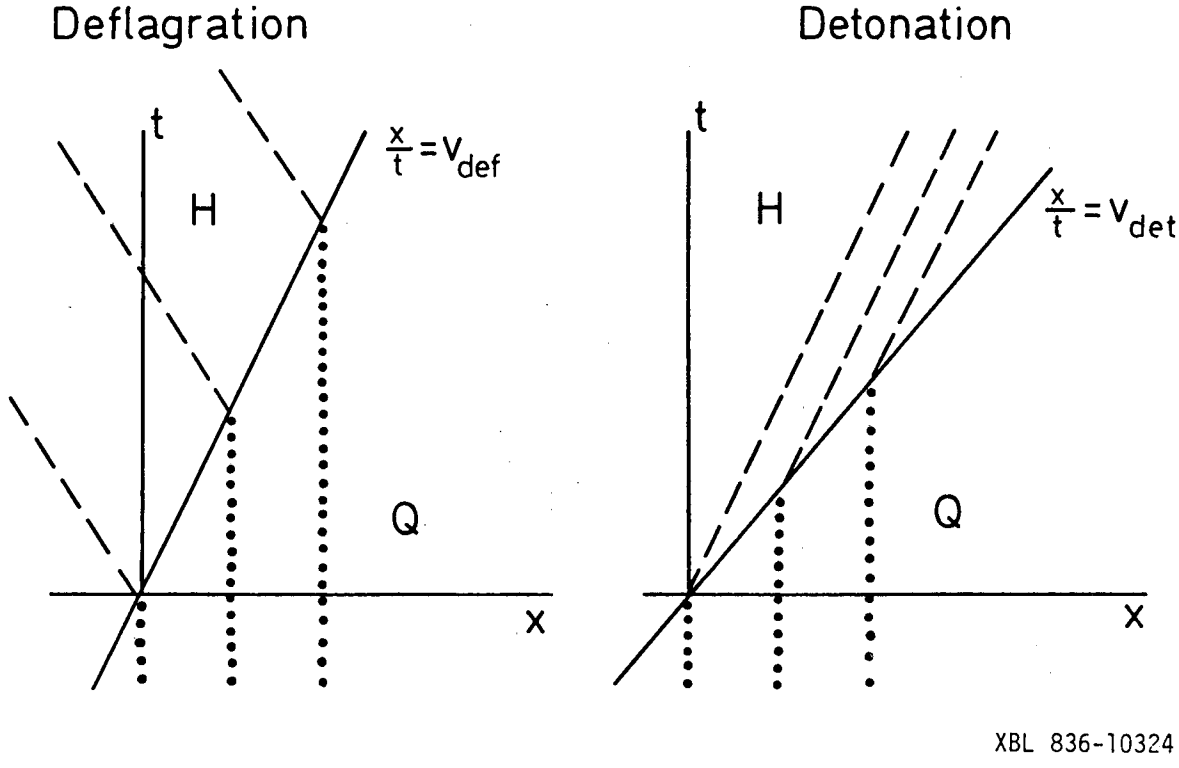
Deflagration
t
H
$\frac{x}{t} = V_{def}$
Q
x
Detonation
t
H
$\frac{x}{t} = V_{det}$
Q
x
XBL 836-10324

Fig. 1

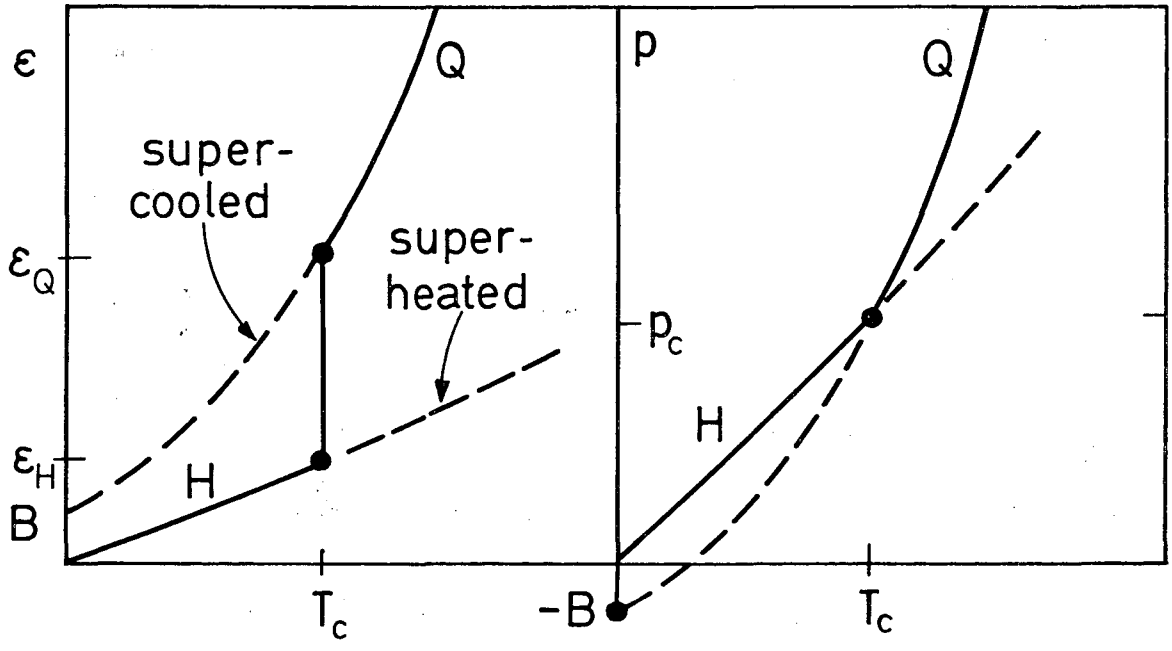

XBL 836-10325

Fig. 2

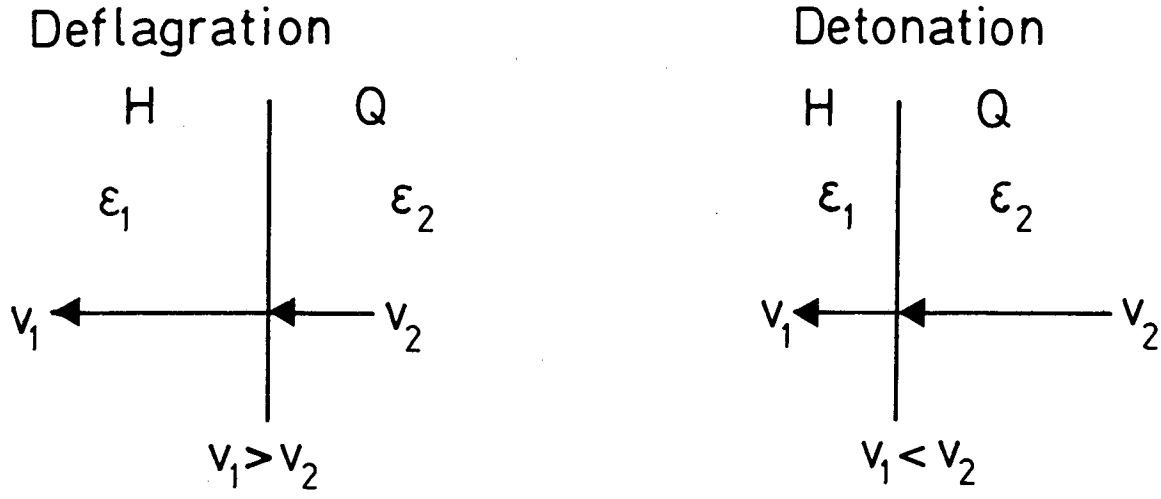

XBL 836-10326

Fig. 3

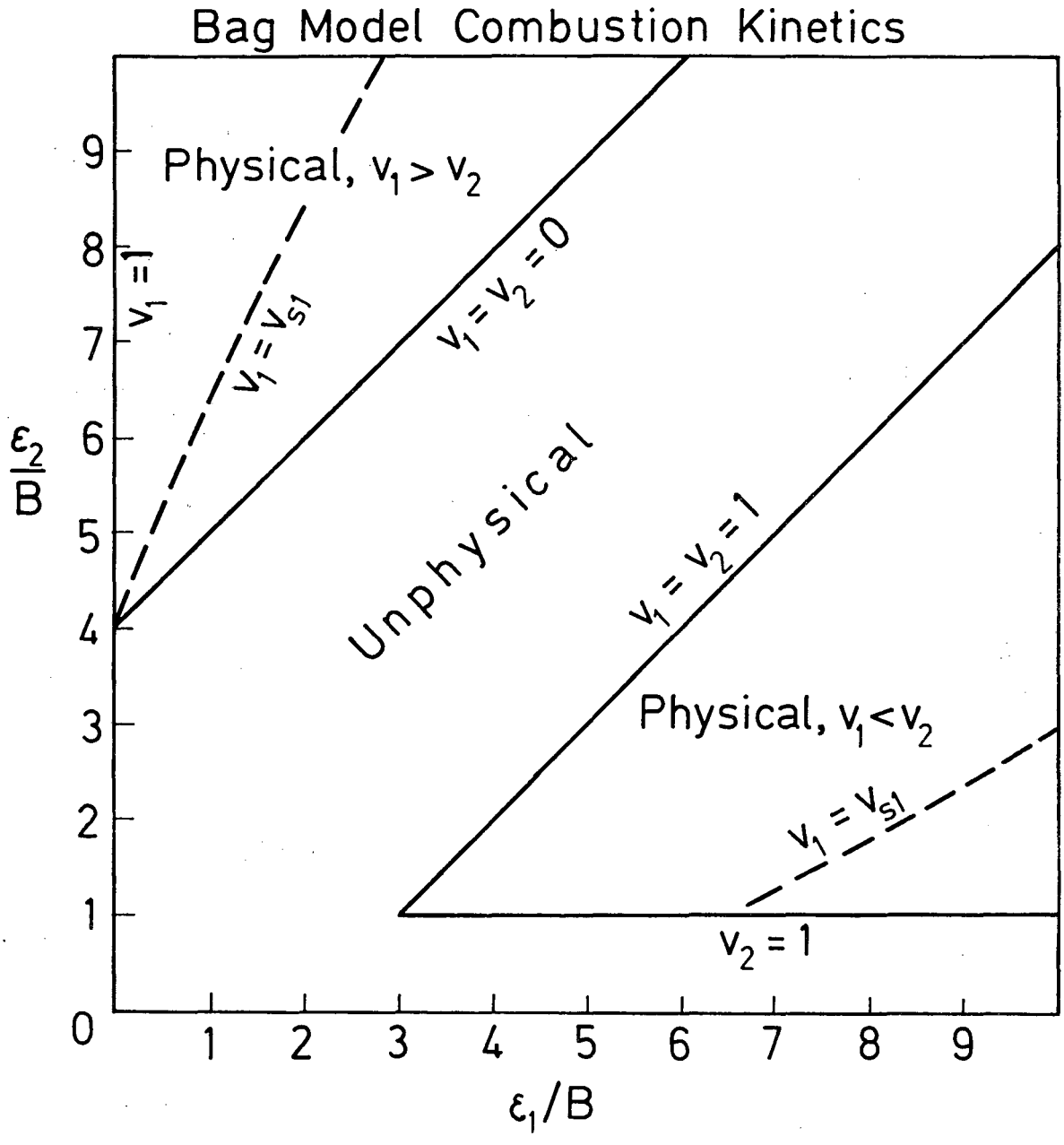

XBL 836-10327

Fig. 4

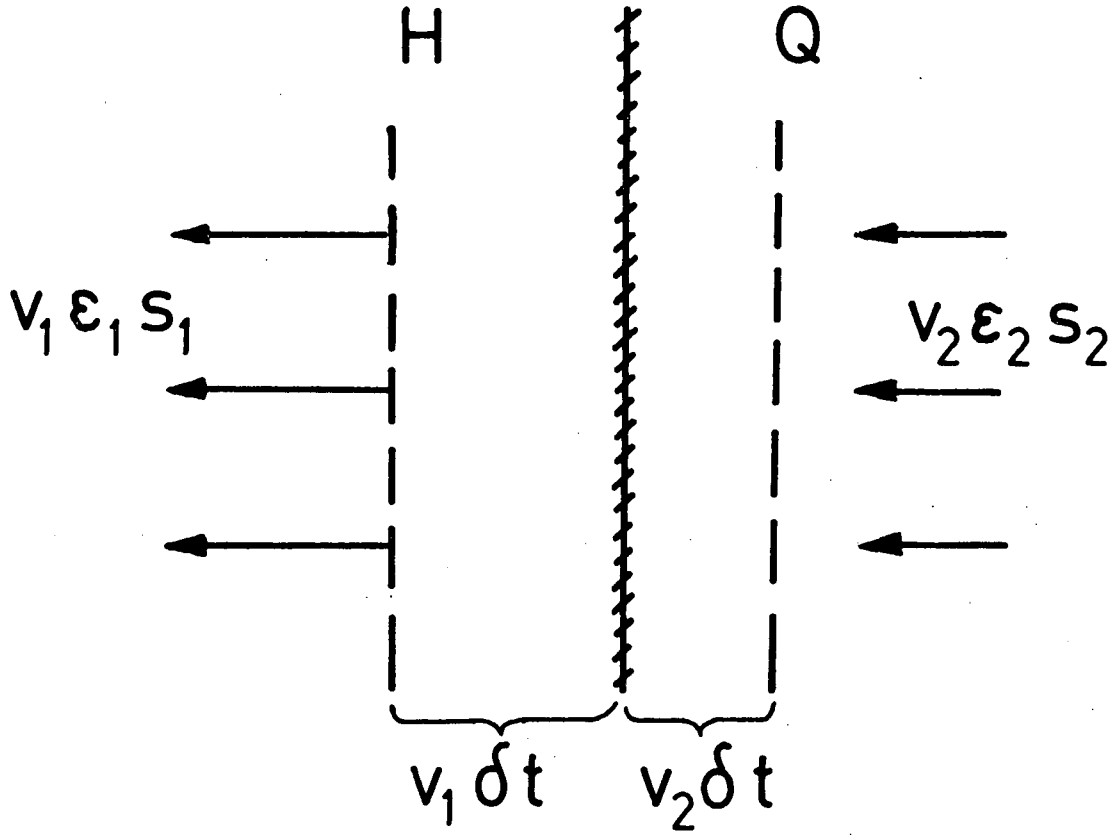

XBL 836-10328

Fig. 5

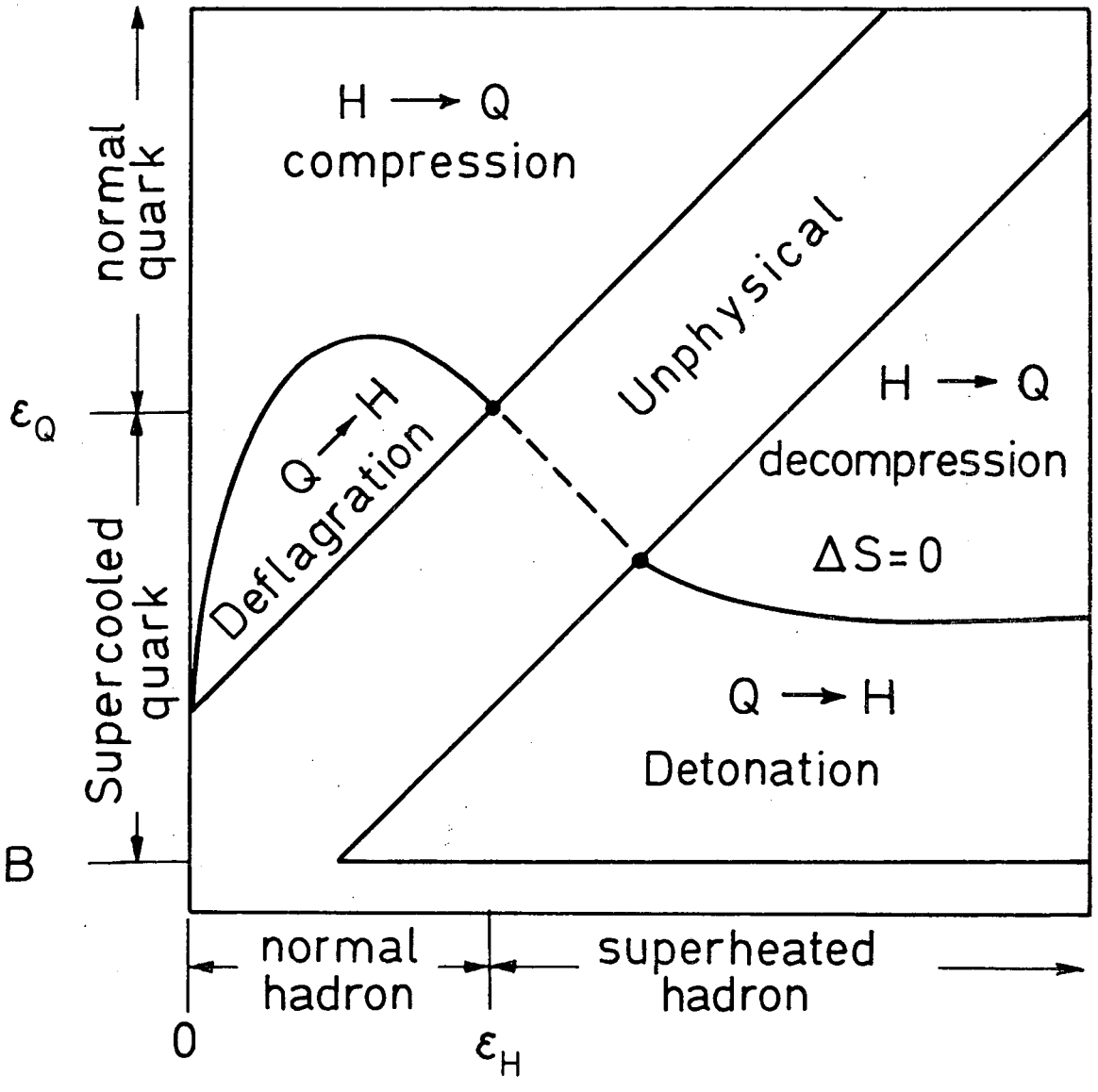

XBL 836-10329

Fig. 6

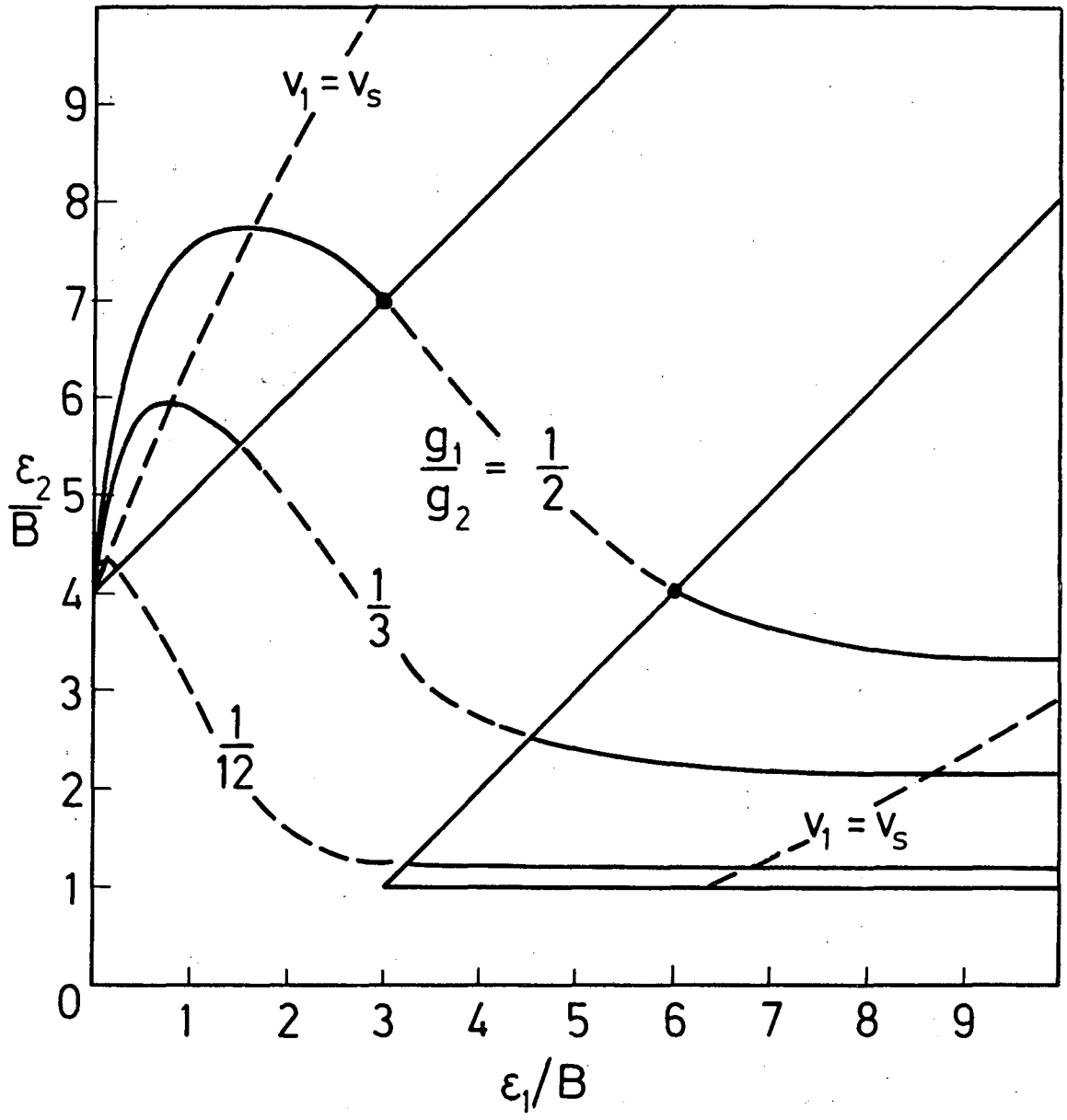

XBL 836-10330

Fig. 7

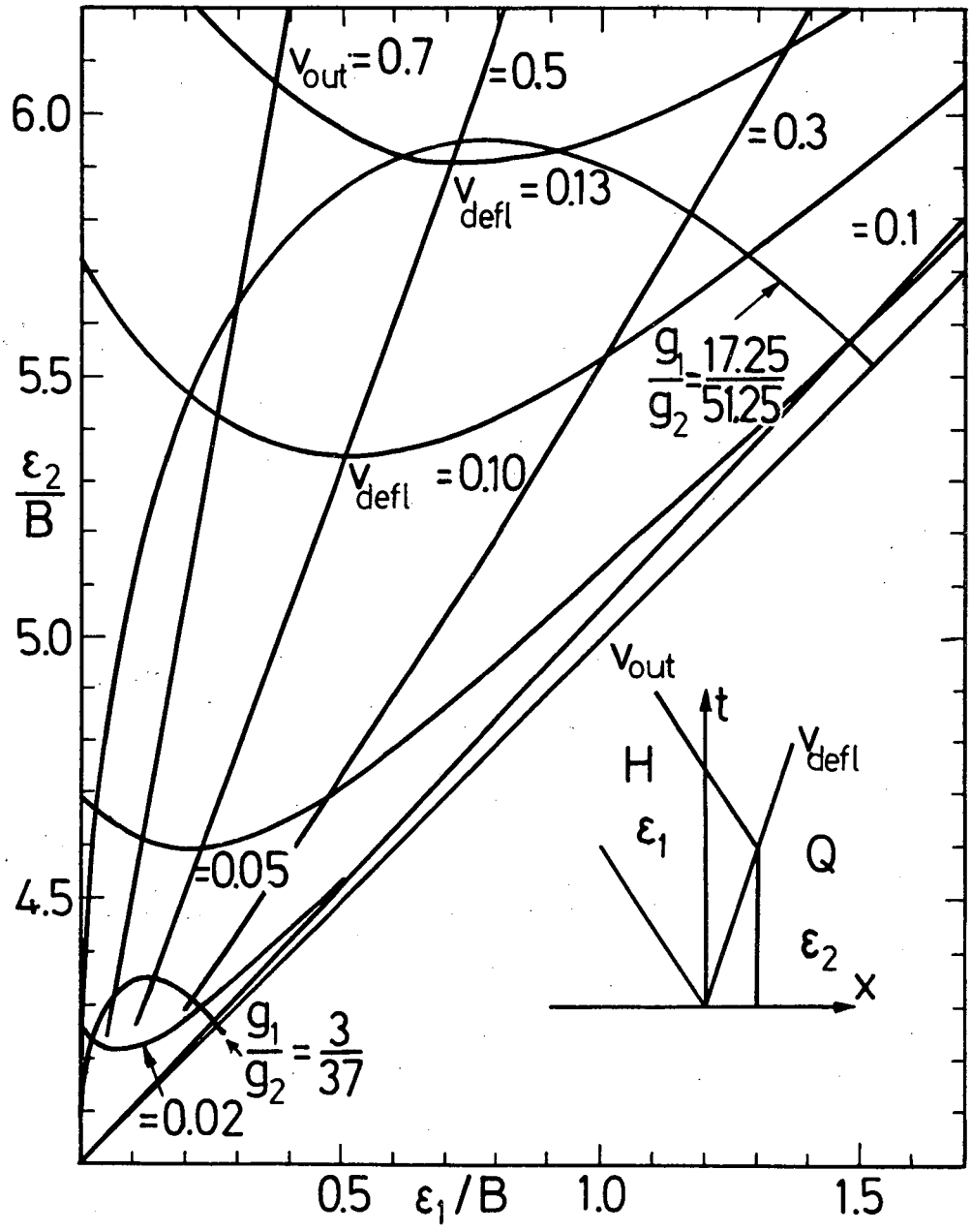

XBL 836-10331

Fig. 8

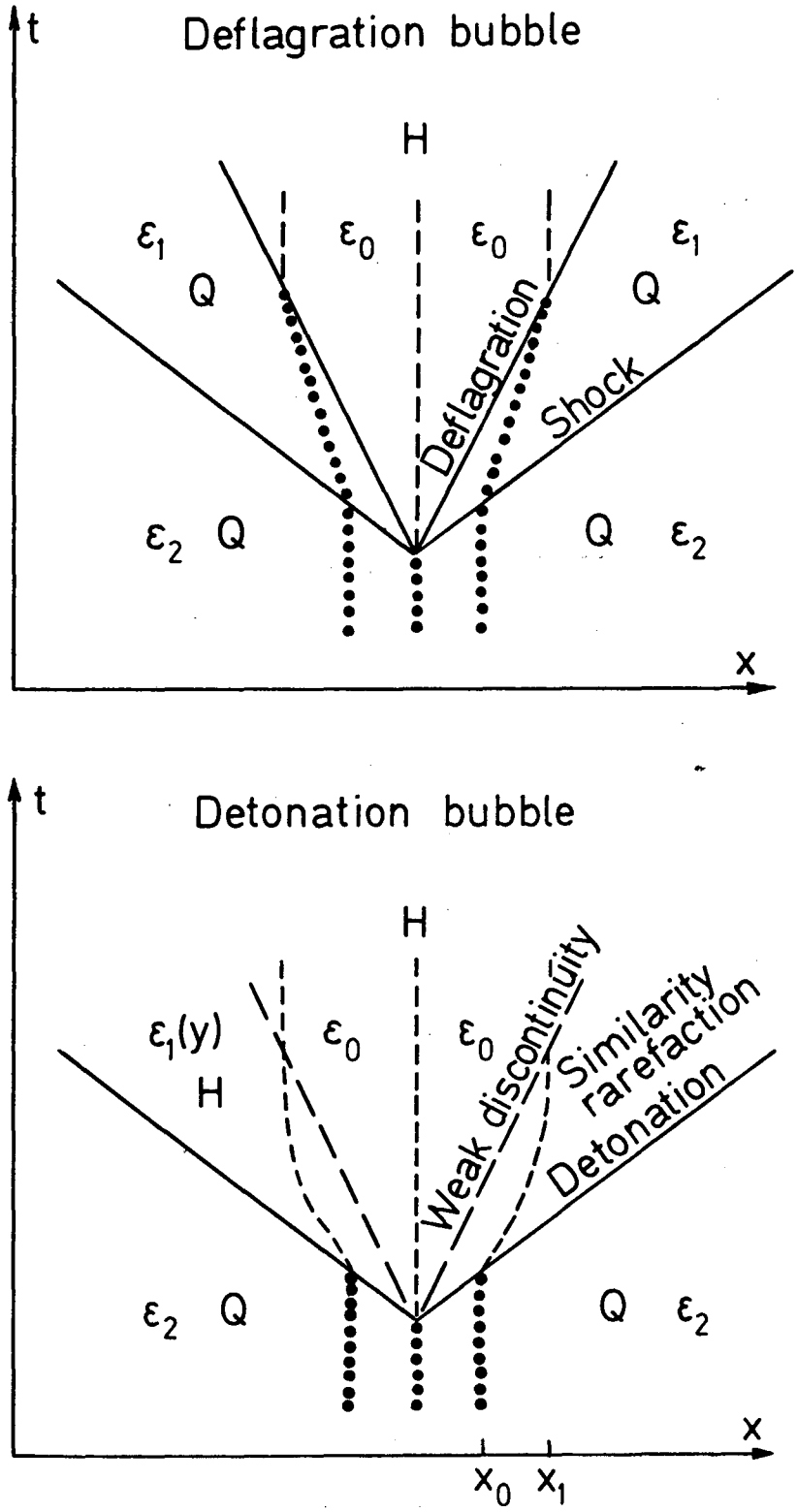

XBL 836-10332

Fig. 9

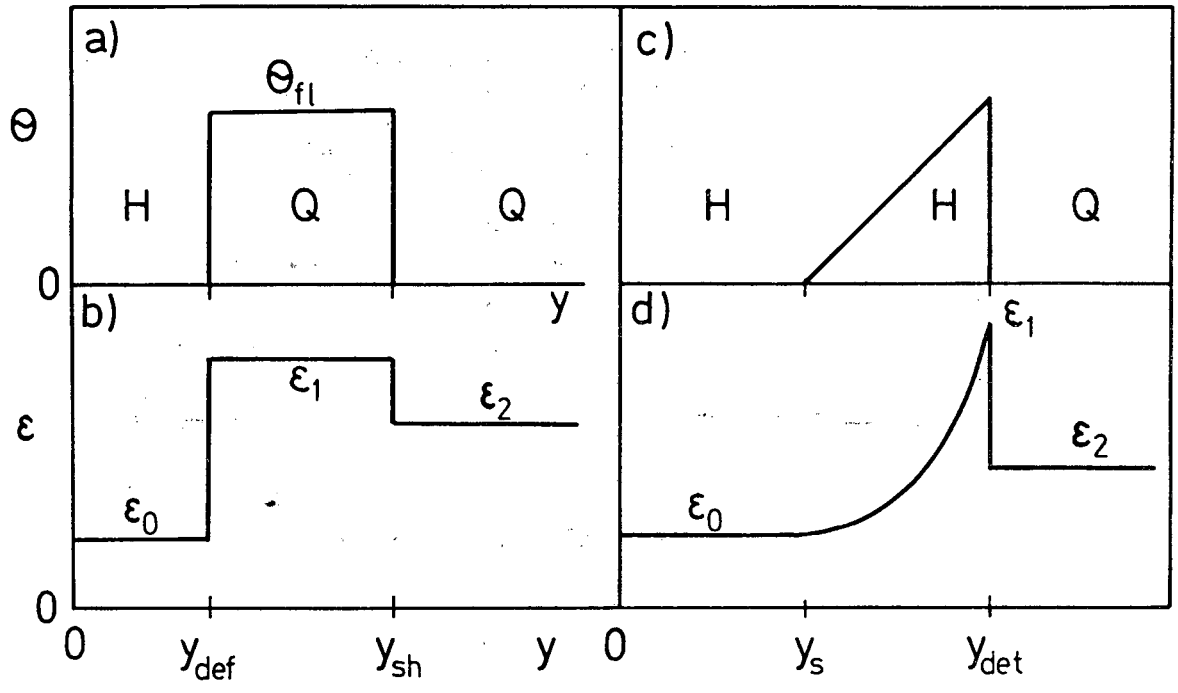

XBL 836-10333

Fig. 10

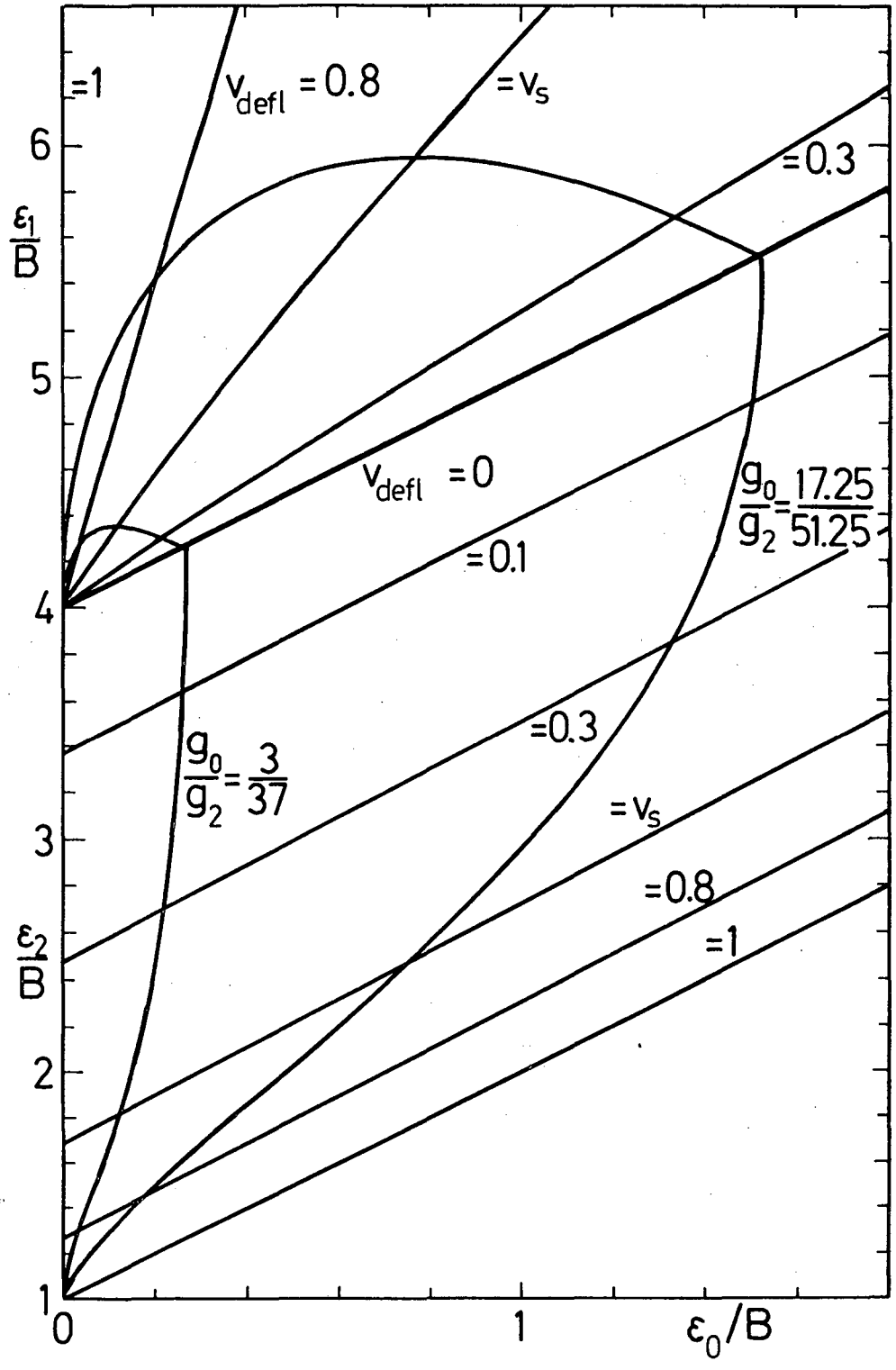

XBL 836-10334

Fig. 11a

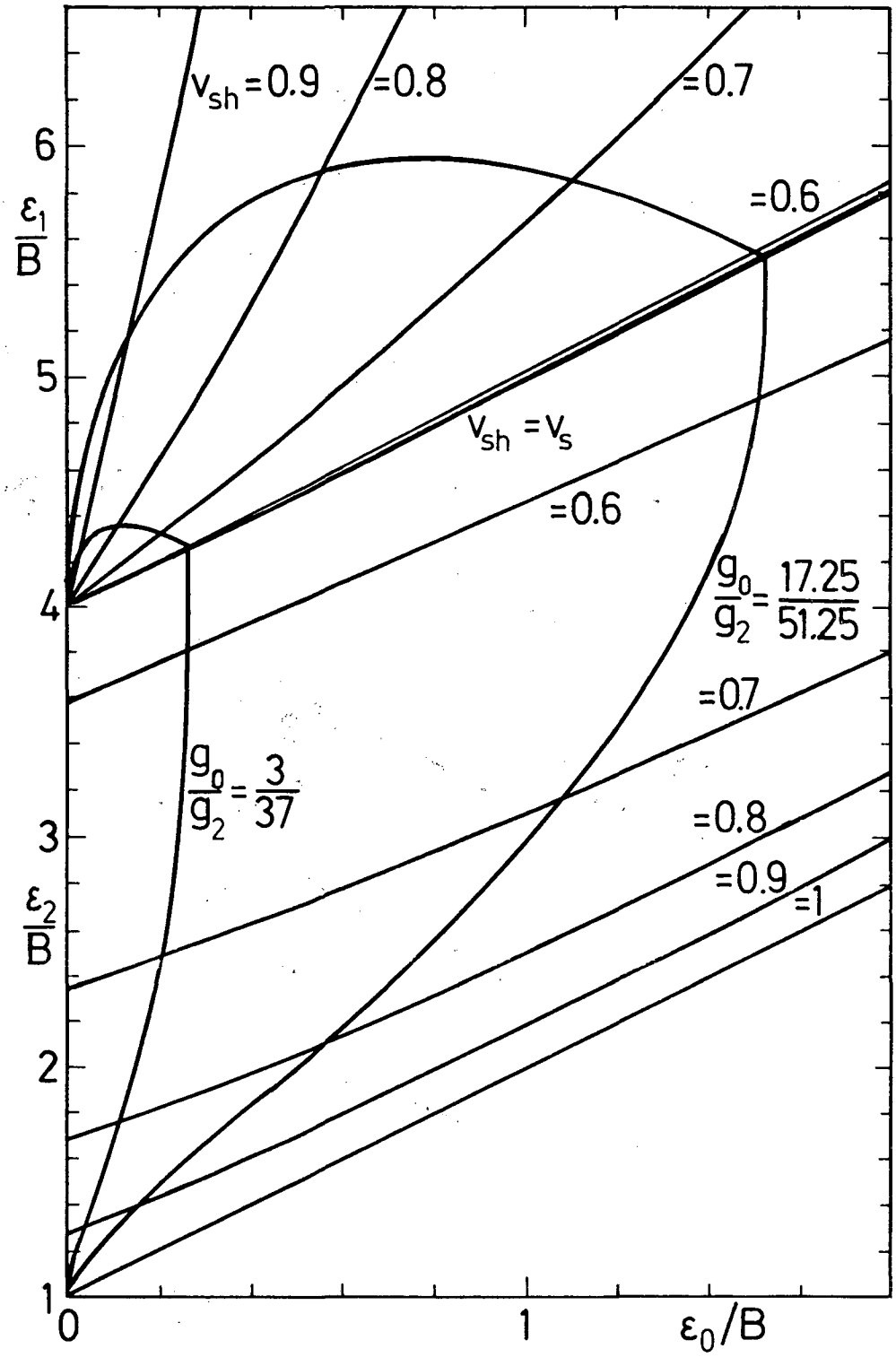

XBL 836-10335A

Fig. 11b

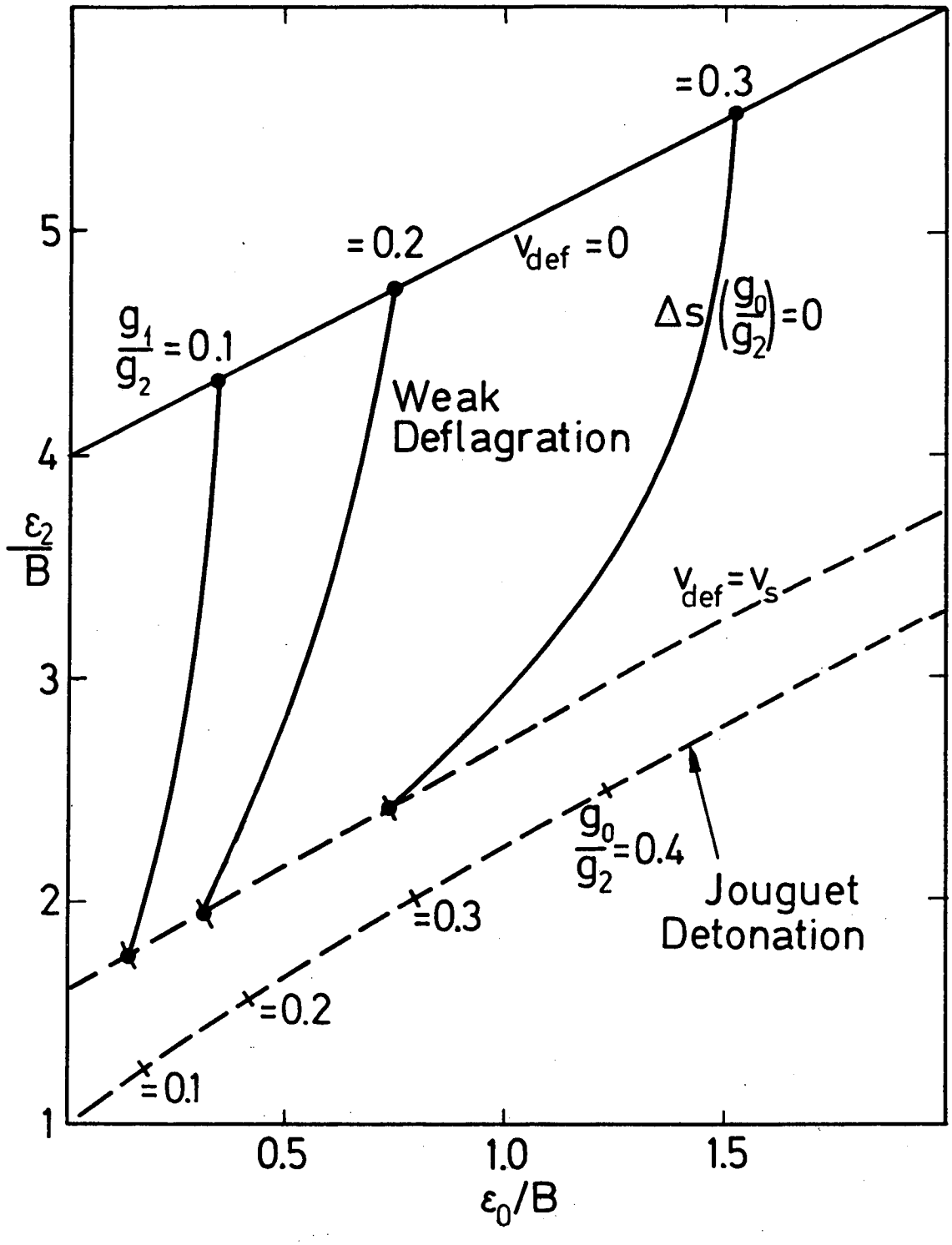

XBL 836-10335

Fig. 12

TECHNICAL INFORMATION DEPARTMENT
LAWRENCE BERKELEY LABORATORY
UNIVERSITY OF CALIFORNIA
BERKELEY, CALIFORNIA 94720